XI International Conference on Computational Plasticity. Fundamentals and Applications
COMPLAS XI
E. Oñate, D.R.J. Owen, D. Peric and B. Suárez (Eds)

DEVELOPMENT OF CRYSTALLOGRAPHIC PROCESS TECHNOLOGY FOR PIEZOELECTRIC ACTUATOR FOR BIO-MEMS DEVICE

EIJI NAKAMACHI*

* Department of Biomedical Engineering
Doshisha University
Kyotanabe, Kyoto 610-0394, Japan
e-mail: enakamac@mail.doshisha.ac.jp, http//biomate.doshisha.ac.jp

Key words: Computational Plasticity, Forming Process, Composites, Nano-mechanics.

Abstract. Recently, the lead free piezoelectric material, which could be used for the actuator and the sensor of medical care devices, such as the health monitoring system (HMS) and the drug delivery system (DDS), is strongly required. In this study, we try to find a new biocompatible and lead-free piezoelectric material, by using the three-scale process-crystallographic analyses scheme, which consists of the first-principles calculations, the homogenization based finite element method, and the process optimization algorithm. After numerical calculations, we found an optimum biocompatible element combination and a tetragonal crystal structure of candidate material $MgSiO_3$. As a result of process crystallography simulation to adjust with the selected substrate Au(111), lattice parameters of $MgSiO_3$ with tetragonal structure were obtained as a=b=0.3449nm and c=0.3538nm, and its aspect ratio was 1.026. The piezoelectric stress constants of a non constraint $MgSiO_3$ crystal, e_{33}=4.57C/m^2, e_{31}=-2.20C/m^2 and e_{15}=12.77C/m^2, were obtained. Macro homogenized piezoelectric stress constants of $MgSiO_3$ thin film were obtained as e_{33}=5.10C/m^2, e_{31}=-3.65C/m^2 and e_{15}=3.24C/m^2. We confirmed the availability of our process crystallographic simulation scheme for a new biocompatible piezoelectric material design through the comparison with the experimental observation of a newly generated $MgSiO_3$ thin film material.

1 INTRODUCTION

Recently, the lead-based piezoelectric materials, such as $PbTiO_3$ and $Pb(Zr,Ti)O_3$, have been applied to various actuators [1] and sensors [2] in Micro Electro Mechanical System (MEMS) devices due to their high piezoelectric and dielectric properties. However, these materials contain the lead. Recently, lead and hazardous material are prohibited to use by Restriction of Hazardous Substances (RoHS) regulation [3]. Recently, the lead-free and biocompatible piezoelectric materials for Bio-MEMS devices have been developed by using the computational and the experimental approaches [4].

Zhang S. et al. [5] doped Ca and Zr in $BaTiO_3$ and succeeded in generating the piezoelectric material with high piezoelectric and dielectric constants. Fu P. et al. [6] doped La_2O_3 in Bi based $(Bi_{0.5}Na_{0.5})_{0.94}Ba_{0.06}TiO_3$ and succeeded in generating the piezoelectric

material with high piezoelectric constant and spontaneous polarization. However, these materials had problem of biocompatibility, and were not adequate for Bio-MEMS devices. Especially, ions of the composition element of a piezoelectric material invade the human body, when piezoelectric materials are applied to the implanted Bio-MEMS device. Therefore, piezoelectric materials should be constructed by biocompatible elements.

In previous study, we have developed a new three-scale analysis algorithm for a new piezoelectric material design, which consists of the first-principles calculation [7] and the process-crystallographic analyses scheme [8]. $MgSiO_3$, which was a candidate for a new biocompatible piezoelectric material and had the perovskite tetragonal structure, was found by using this numerical scheme, and it showed a high piezoelectric constant. Before a new material $MgSiO_3$ design and generation, we confirm the availability of our newly developed simulation scheme to analyze the epitaxial growth process of the perovskite tetragonal crystal structure and the piezoelectric properties of the existence piezoelectric material $BaTiO_3$. Numerical results showed a good agreement with the experimental ones.

In this study, we apply our three-scale process-crystallographic analyses scheme to design a new biocompatible $MgSiO_3$ piezoelectric thin film. Then, this thin film is generated by using the radio-frequency (RF) magnetron sputtering. Finally, the crystallographic orientation and the piezoelectric strain constant d_{33} are measured by using the X-ray diffracto-meter (XRD) and the ferroelectric measurement system to confirm the availability of our process-crystallographic design algorithm.

2 FIRST-PRINCIPLES AIDED THREE-SCALE ANALYSIS

2.1 Three-scale modeling of a piezoelectric thin film

Figure 1 shows the schematic description of the first-principles aided three-scale modeling of the piezoelectric thin film, which is grown on a substrate. It shows the three-scale structures, such as a “crystal structure”, a “micro structure” and a “macro structure.”

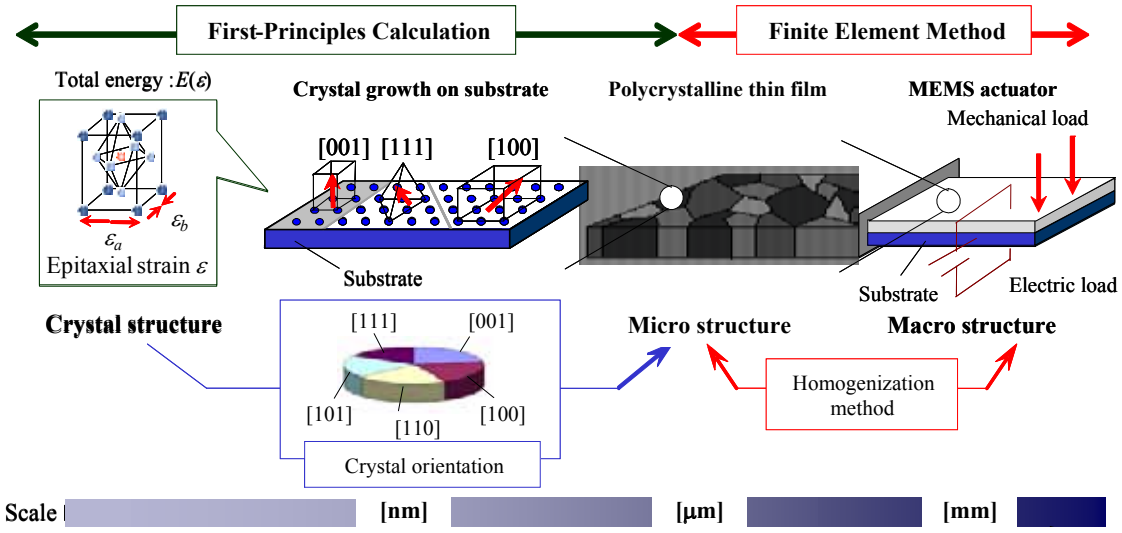

Figure 1: First-principles aided three-scale modeling of piezoelectric thin film on substrate

In the crystal structure scale, the stable structure and the crystal properties are evaluated by using the first-principles calculation. Next, the preferred orientations and their fractions are determined by considering the epitaxial strains, caused by the lattice mismatches between the thin film and the substrates. Additionally, the calculated crystal morphology is introduced into the micro structure and properties of the macro structure, which consist the thin film and the substrate, are calculated by the two-scale finite element analysis, which is derived based on the homogenization theory.

2.2 Process crystallography simulation algorithm

Thin film crystal is strained by mismatch between lattice constant of thin film and one of substrate, when thin film is grown epitaxially. Virtual crystal clusters with various orientations and conformations are generated by our process crystallography simulation, because thin film crystal has various conformations on a substrate as shown in Figure 2(a) and (b). Total energies of virtual clusters are varied by the crystal strain. Therefore, total energies of strained crystals are calculated by using the density functional theory (DFT), and total energies of virtual clusters are calculated. Total energies of virtual clusters are compared with one of stable state and total energy increments of virtual crystals are also calculated. In order to calculate the possibility of growth of the virtual cluster P_i, total energy increment ΔE is introduced into the canonical distribution as flows:

$$P_i = \frac{\exp[\Delta E_i / k_B T]}{\sum_n \exp[\Delta E_n / k_B T]} \tag{1}$$

where, k_B is the Boltzmann constant and T the absolute temperature.

The existing lead-free $BaTiO_3$ piezoelectric material with (111) orientation, which has perovskite type tetragonal structure as same as $MgSiO_3$, shows highest piezoelectric properties. In this study, we find the best substrate of $MgSiO_3$(111) with the minimum energy is found.

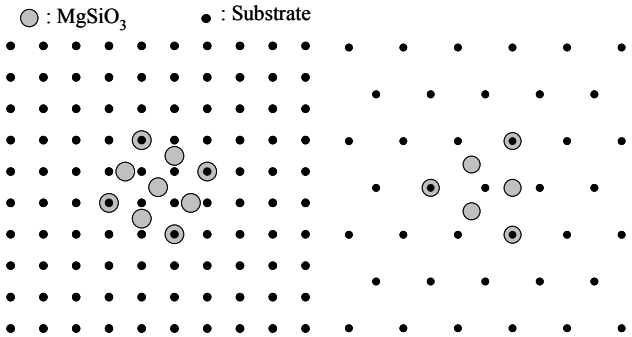

(a) $MgSiO_3$/Mo(100) (b) $MgSiO_3$/Au(111)

Figure 2: Schematic diagram for some conformations of $MgSiO_3$ crystal cluster on substrates

2.3 Numerical characterization process of the macro homogenized piezoelectric thin film

In order to evaluate the macro homogenized properties of the thin film, the micro structure of the thin film with a preferred orientation is applied to the two-scale finite element analysis on basis of crystallographic homogenization theory as shown in Fig.1. The crystal orientation fraction of the thin film is determined by frequency distribution of each grown cluster, which is calculated by the canonical distribution. The crystal orientation is introduced in the micro structure. For simplicity, the micro structure is divided evenly by eight-node rectangular solid elements and crystal orientations are assigned at the integration points of each element. For $BaTiO_3$, we employ experimentally obtained properties in the micro structure, and for $MgSiO_3$, computational properties obtained by the first-principles are employed for the micro structure.

3 DESIGN OF A NEW BIOCOMPATIBLE MATERIAL

3.1 The first-principles calculation

To calculate the crystal structure of perovskite $MgSiO_3$, energy cutoff was set as 500eV and k-point was generated by 8×8×8 Monkhurst-Pack mesh. We calculated the cubic structure as shown in Figure 3. Lattice constants a=b=c=0.3459nm were obtained.

The eigenfrequency of the cubic structure of $MgSiO_3$ was obtained as -112cm^{-1} by using phonon vibration analysis. This result indicated that $MgSiO_3$ crystal had possibility of phase transition to another phase, due to the eigenfrequency with negative value. Table I shows eigenvectors of each atom. It indicated that $MgSiO_3$ cubic crystal had possibility to change to the tetragonal structure, because all eigenvectors were existed along c axis only.

In order to calculate the stable tetragonal structure, initial structure was determined by employing eigenvectors. As a result, lattice parameters were obtained as a=b=0.3449nm and c=0.3538nm. The aspect ratio a/c=1.026 was obtained from 1.011 of $BaTiO_3$ thin film [9] to 1.049 of $PbTiO_3$ thin film [10]. Table 2 shows internal coordinates of the tetragonal $MgSiO_3$. We obtained reasonable result, because displacements of all internal atoms of the tetragonal structure had good agreement with direction of eigenvectors of the cubic structure as show in Table 1.

Furthermore, the variation of polarization and piezoelectricity of $MgSiO_3$ caused by the assigned small strain was calculated. The piezoelectric stress constants of $MgSiO_3$ crystal were determined as e_{33}=4.57C/m^2, e_{31}=-2.20C/m^2 and e_{15}=12.77C/m^2.

3.2 Determination of the best substrate

Biocompatible elements have bio-essential elements (Ca, Fe, Ge, Mg, Mn, Mo, Na, Ni, Sn and Zn) and elements (Si, Ta, Ti and Zr), which have been used in the human body. In previous study, we calculated reactivity with biological molecules and found new biocompatible elements (Li, Ba, K, Au, Rb, In) [11]. In these 20 biocompatible elements, we selected Au, Mo and Ta for candidates of the substrate, because these elements satisfied four terms, such as (1) the melting point is over sputtering temperature, (2) element dose not react to other elements under sputtering condition, (3) element is able to be use the under electrode and (4) element is cubic structure. Lattice parameters of Au with FCC cubic structure are

a=b=c=0.4080nm, ones of Mo with BCC cubic structure are a=b=c=0.3147nm and ones of Ta with BCC cubic structure are a=b=c=0.3289nm.

Table 3 shows result of crystallography simulation on (100), (110) and (111) oriented three substrate candidates. Total energies and orientation fractions of epitaxially grown $MgSiO_3$ thin films were different depend on conformations as shown in Figure 4. It shows an example of conformations of $MgSiO_3$(001)/Au(100).

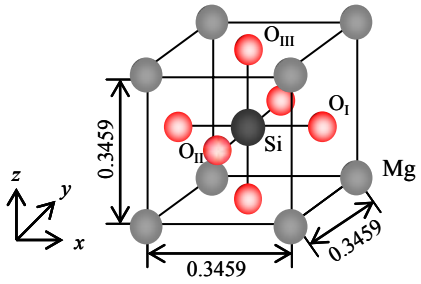

Figure 3: Schematic diagram for some conformations of $MgSiO_3$ crystal cluster on substrates

Table 1: Eigenvectors of interior atoms in $MgSiO_3$ Crystal

Atom	Eigenvector		
	ξ_x	ξ_y	ξ_z
Mg	0.00	0.00	0.88
Si	0.00	0.00	-0.13
O_I	0.00	0.00	-0.37
O_{II}	0.00	0.00	-0.37
O_{III}	0.00	0.00	-0.22

Table 2: Internal coordinates of $MgSiO_3$ crystal

Atom	x	y	z
Mg	0.00	0.00	0.00
Si	0.50	0.50	0.42
O_I	0.00	0.50	0.38
O_{II}	0.50	0.00	0.38
O_{III}	0.50	0.50	0.90

Table 3: Internal coordinates of $MgSiO_3$ crystal

Substrate		$MgSiO_3$		
Atom	Facet	Facet	Energy [eV]	Fraction [%]
Au	(100)	(001)	0.075	87.7
		(001)	0.126	12.3
	(110)	(101)	0.343	92.0
		(101)	0.406	8.0
	(111)	(111)	0.539	100.0
Mo	(100)	(100)	0.093	61.5
		(001)	0.105	38.5
	(110)	(001)	0.254	70.1
		(001)	0.287	20.2
		(101)	0.305	9.7
	(111)	(111)	0.774	100.0
Ta	(100)	(001)	0.001	90.8
		(001)	0.061	9.1
		(001)	0.172	0.1
	(110)	(101)	0.329	99.8
		(101)	0.488	0.2
	(111)	(101)	0.929	100.0

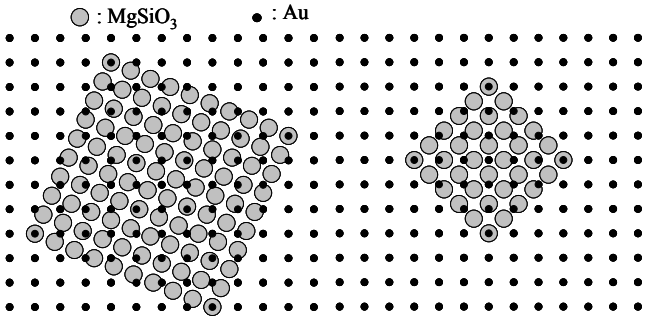

Figure 4: Conformations of $MgSiO_3$/Au(100) calculated by process crystallography simulation

Therefore, we summarized numerical results of independent orientations, total energies and fractions in Table 3. It shows that $MgSiO_3$(111) with highest piezoelectric property could be grown on Au(111) and Mo(111) substrates. Here, Au(111) was the best substrate of biocompatible $MgSiO_3$ thin film, because the total energy of $MgSiO_3$ on Au(111) was smaller than one on Mo(111) substrate.

Finally, the macro homogenized piezoelectric property of $MgSiO_3$ thin film on the best substrate, Au(111), was calculated by using the two-scale finite element analysis on basis of crystallographic homogenization theory. As a result, macro homogenized piezoelectric stress constants were calculated as e_{33}=5.10C/m^2, e_{31}=-3.65C/m^2 and e_{15}=3.24C/m^2.

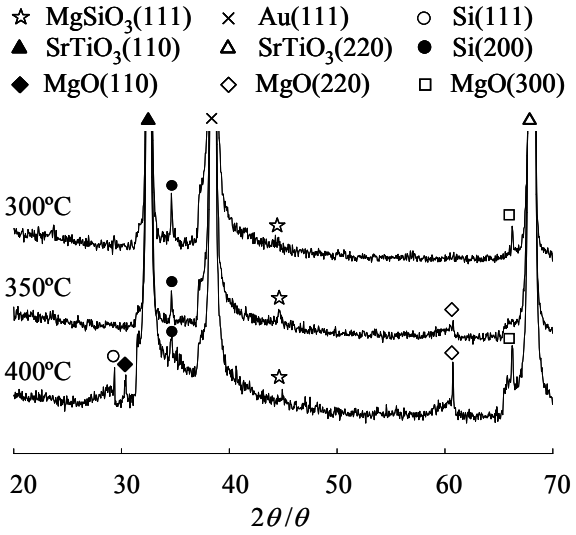

Figure 5: XRD $2\theta/\theta$ patterns for $MgSiO_3$ thin films generated at T_a=650ºC and T_s =300, 350 and 400 ºC

4 EXPERIMENTAL RESULTS OF THIN FILM GENERATION BY SPUTTERING

In order to confirm the availability of our process-crystallographic simulation scheme, $MgSiO_3$ thin film with the perovskite tetragonal crystal structure was generated by using RF

magnetron sputtering apparatus. We employed the simple search algorithm, such as the experimental design algorithm, by employing two design parameters, such as the substrate temperature T_s and post annealing temperature T_a.

Figure 5 shows $2\theta/\theta$ patterns for $MgSiO_3$ thin film generated at T_a=650ºC and T_s =300, 350 and 400 ºC. The peak of MgSiO (111) crystal was obtained.

The displacement-voltage curves were measured by using the ferroelectric measurement system in six cases of combinations with T_a=600, 650 and 700 ºC and T_s =300 and 350 ºC. Figure 6 shows displacement-voltage curves of generated piezoelectric $MgSiO_3$ thin films. It means that all films showed the piezoelectric property because of typical butterfly-type hysteresis curves. The piezoelectric strain constant d_{33} can be calculated by the gradient at cross point of the curve. Figure 7 shows measurement results of d_{33} under conditions of T_s =300, 350 and 400 ºC, and T_a=650 ºC.

Finally, the optimum condition, T_s=300ºC and T_a=650ºC, was found and the piezoelectric strain constant was d_{33}=346.7pm/V.

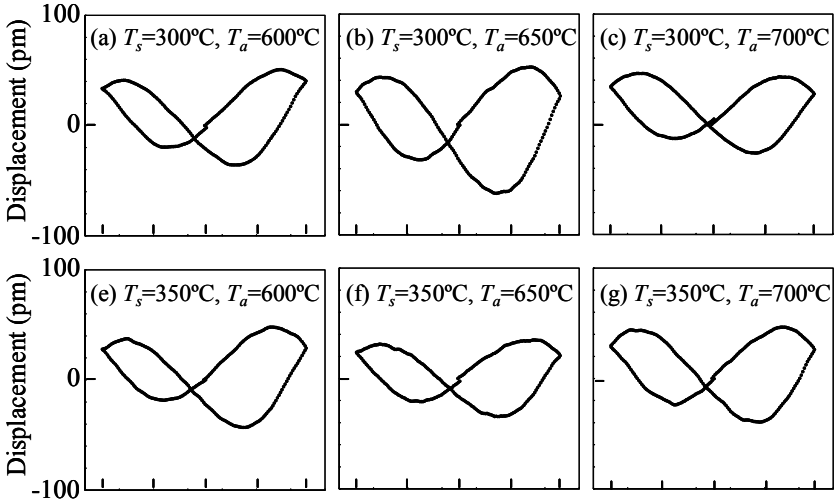

Figure 6: Displacement-voltage curves of $MgSiO_3$ thin film

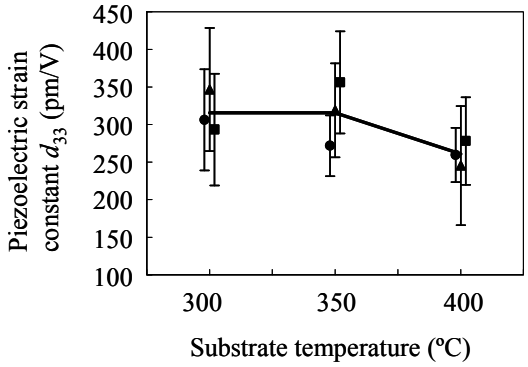

Figure 7: Relationship between piezoelectric strain constant d_{33} and substrate temperature under the condition of the post-anneal temperature 650ºC

5 CONCLUSION

In order to generate a new biocompatible $MgSiO_3$ piezoelectric thin film, which can apply to the Bio-MEMS device, our three-scale process-crystallographic simulation scheme for a new material generation was applied. Further, $MgSiO_3$ was generated by using RF magnetron sputtering apparatus and confirm the availability of our simulation scheme through the comparison with the experimental results. Finally, following results were obtained.

(1) Lattice constants of $MgSiO_3$ with tetragonal structure were obtained as $a=b=0.3449$nm and $c=0.3538$nm, and its aspect ratio is 1.026.
(2) The piezoelectric stress constants of $MgSiO_3$ crystal, $e_{33}=4.57C/m^2$, $e_{31}=-2.20C/m^2$ and $e_{15}=12.77C/m^2$, were obtained.
(3) Au(111) was the best biocompatible substrate, on which $MgSiO_3$(111) thin film with minimum total energy can be grown.
(4) Macro homogenized piezoelectric stress constants of $MgSiO_3$ thin film on Au(111) substrate were obtained as $e_{33}=5.10C/m^2$, $e_{31}=-3.65C/m^2$ and $e_{15}=3.24C/m^2$.
(5) An optimum condition was obtained as T_s=300ºC and T_a=650ºC, and its piezoelectric strain constant was $d_{33}=346.7$pm/V.

Consequently, we indicated that a new biocompatible $MgSiO_3$ thin film could be applied to actuators and sensors in Bio-MEMS.

ACKNOWLEDGEMENTS

I gratefully appreciate Ph. D. Hwisim Hwang for his analytical and experimental works on this subject. Further, I would like to acknowledge the financial support of the Grant-in-Aid for Scientific Research (B) (23360059) by the Ministry of Education, Culture, Sports, Science and Technology of Japan.

REFERENCES

[1] Tsai, J.Z., Chen, C.J. , Chen, W.Y., Liu, J.T., Liao, C.Y. and Hsin, Y.M. A new PZT piezoelectric sensor for gravimetric applications using the resonance-frequency detection. *Sens. Act. B.* (2009) **139**:259-264.
[2] Watson, B. , Friend, J. and Yeo, L. Piezoelectric ultrasonic micro/milli-scale actuators. *Sens. Act. A*. (2009) **152**:219-233.
[3] European Parliament, On the restriction of the use of certain hazardous substances in electrical and electric equipment. *Official J. Eur. Union.* (2003) **37**:19-23.
[4] Lin, D., Kwok, K.W. and Chan, H.L. Dielectric and piezoelectric properties of $K_{0.5}Na_{0.5}NbO_3$-$AgSbO_3$ lead-free ceramics. *J. Appl. Phys.* (2009) **106**:034102.1-034102.5.
[5] Zhang, S.W., Zhang, H., Zhang, B.P. and Zhao, G. Dielectric and piezoelectric properties of $(Ba_{0.95}Ca_{0.05})(Ti_{0.08}Zr_{0.12})O_3$ ceramics sintered in a protective atmosphere. *J. Eur. Ceram. Soc.* (2009) **29**:3235-3242.
[6] Fu, P., Xu, Z., Chu, R., Li, W., Zhang, G. and Hao, J. Piezoelectric, ferroelectric and dielectric properties of La_2O_3-doped $(Bi_{0.5}Na_{0.5})_{0.94}Ba_{0.06}TiO_3$ lead-free ceramics. *Mater. Des.* (2009) **31**:796-801.
[7] Uetsuji, Y., Hwang, H., Tsuchiya, K. and Nakamachi, E. First-principles study on crystal structure and piezoelectricity of perovskite-type silicon oxides. *J. Solid Mech. Mater. Eng.* (2008) **2**:1427-1435.

[8] Hwang, H., Uetsuji, Y., Sakata, S., Tsuchiya, K. and Nakamachi, E. Crystal growth prediction by first-principles calculations for epitaxial piezoelectric thin films. *J. Comput. Sci. Technol.* (2009) **3**:267-274.
[9] Schubert, J., Siegert, M., Faradmanesh, M., Zander, W., Prompers, M., Buchal, C., Lisoni, J. and Lei, C.H. Superconducting and electro-optical thin films prepared by pulsed laser deposition technique. *Appl. Surf. Sci.* (2000 **168**:208-214.
[10] Satoh, T., Wasa, K., Tabata, K., Adachi, H., Ichilawa, Y. and Setsune, K., Microstructures of sputtered $PbTiO_3$ thin films. *J. Vac. Sci. Technol. A*. (1995) **13**:1022-1026.
[11] Parr, R.G. and Pearson, G. Absolute hardness: companion parameter to absolute electronegativity. *J. Am. Chem. Soc.* (1983) **105**:7512-7516.